Physical Modeling of Substrate Resistance in RF MOSFETs

Jeonghu Han, Minkyu Je, and Hyungcheol Shin

Dept. of EECS, Korea Advanced Institute of Science and Technology,
373-1 Guseong-dong, Yuseong-gu, Daejon 305-701, Korea, inflames@inca.kaist.ac.kr

ABSTRACT

A simple and accurate method is presented for extracting the substrate resistance of RF MOSFETs. The extraction results for 0.18 μm MOSFETs are shown for various bias conditions. The dependence of the extracted substrate resistances on the device geometry is also presented. The substrate signal coupling effect on the small-signal output admittance and its gate-bias dependence are analyzed.

Keywords: RF MOSFET, MOSFET modeling, substrate resistance, substrate coupling, parameter extraction

1 INTRODUCTION

Recent RF MOSFET models include the substrate-related components such as the substrate resistance (R_{sub}), since the substrate resistance significantly affects the small-signal output characteristics of RF MOSFETs at high frequencies [1]-[4]. The four-terminal MOSFET with substrate parasictics has significant signal coupling through the substrate *R-C* network. It is crucial for MOSFET modeling and RF IC design to extract and predict the substrate resistance of a MOSFET accurately as a function of the bias and the device layout geometry. In this paper, we present a simple and accurate method for extracting the R_{sub} of RF MOSFETs. Using the technique, the bias dependence and the layout geometry dependence of R_{sub} were extracted and presented. Also, we analyzed the substrate signal coupling effect on the small-signal output admittance and its gate-bias dependence accurately.

2 EXTRACTION METHOD OF R_{sub}

The effect of substrate parasitics can be accurately described by a simple subcircuit extension of the conventional MOSFET model by using a single lumped substrate resistance R_{sub} [5]. When the gate voltage V_{gs} is smaller than the threshold voltage V_{th}, most intrinsic components of a MOSFET are negligible and the equivalent circuit of an RF MOSFET is simplified as the one presented in Fig. 1. C_{gs0} and C_{gd0} represent the gate-to-source and the gate-to-drain zero-bias capacitances, respectively. C_{gb} indicates the sum of the intrinsic and the extrinsic gate-to-body capacitances and C_{js} and C_{jd} are the source and the drain junction capacitances. R_{poly} and R_{sub} represent the gate and the substrate resistances. From the equivalent circuit in Fig. 1, some of the *Y*-parameters are given by equations (1)-(5) up to a few GHz.

$$\mathrm{Re}[Y_{11}] \approx \omega^2 R_{poly}(C_{gs0} + C_{gd0} + C_{gb})^2 + \omega^2 R_{sub} C_{gb}^2 \quad (1)$$

$$\mathrm{Im}[Y_{11}] \approx \omega(C_{gs0} + C_{gd0} + C_{gb}) \quad (2)$$

$$\mathrm{Im}[Y_{12}] \approx -\omega C_{gd0} \quad (3)$$

$$\mathrm{Re}[Y_{22}] \approx \omega^2 R_{sub} C_{jd}^2 + \omega^2 R_{poly} C_{gd0}^2 \quad (4)$$

$$\mathrm{Im}[Y_{22}] \approx \omega(C_{jd} + C_{gd0}) \quad (5)$$

Using (1)-(5), we can extract C_{gd0}, C_{gb}, C_{jd}, R_{poly}, and R_{sub} from the measured *Y*-parameters.

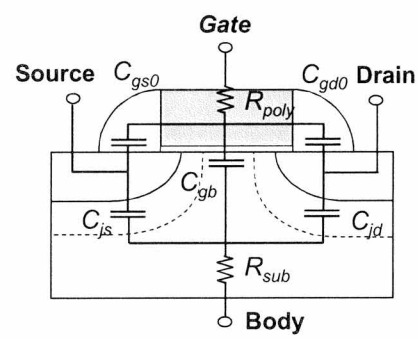

Fig. 1. Equivalent circuit of an RF MOSFET when the device is turned off and the intrinsic components of the MOSFET are negligible. The substrate is represented by a single lumped resistor R_{sub}.

The MOSFETs were fabricated in a commercially available 0.18-μm CMOS technology. The *S*-parameters of 0.18-μm nMOSFETs were measured using an Agilent 8510C network analyzer and a CASCADE Summit probe station. Open and short dummy patterns were used to deembed the pad parasitics.

3 BIAS DEPENDENCE OF R_{sub}

C_{jd} and R_{sub} at various gate voltages are illustrated in Fig. 2. When V_{gs} increases to near V_{th}, the intrinsic components of the MOSFET become significant, which makes the equivalent circuit in Fig. 1 and its corresponding parameters invalid. Therefore, it is recommended that the C_{jd} and R_{sub} should be extracted at V_{gs} smaller than about (V_{th} – 0.3 V). The extraction of R_{sub} at V_{gs} < (V_{th} – 0.3 V), or simply at V_{gs} = 0 V gives a quite proper value because R_{sub} has a very weak gate-bias dependence as shown in Fig. 2 [6].

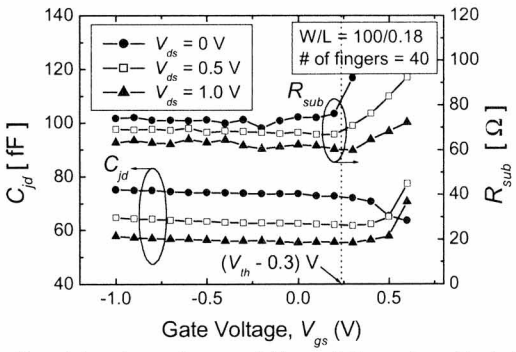

Fig. 2. Gate bias dependence of C_{jd} and R_{sub} when V_{ds} is 0 V, 0.5 V, and 1.0 V.

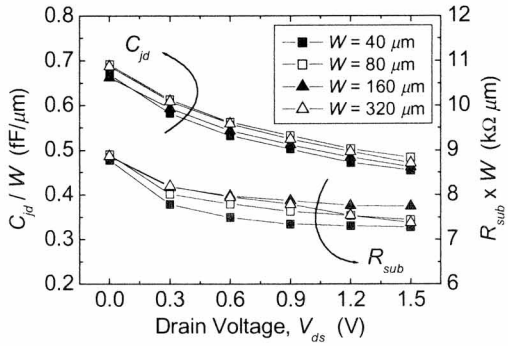

Fig. 3. Drain bias dependence of C_{jd} and R_{sub} when extracted at V_{gs} = 0 V.

The drain-bias dependence of C_{jd} and R_{sub} are presented in Fig. 3. C_{jd} and R_{sub} were extracted for the devices with various channel widths: 40, 80, 160, and 320 μm. As the drain bias increased, C_{jd} decreased as expected. Fig. 3 shows that R_{sub} also decreased when the drain voltage increased because the path between the intrinsic body and the (external) body contacts becomes shorter with widening of the depletion region.

4 GEOMETRY DEPENDENCE OF R_{sub}

The values of R_{sub} were extracted for NMOSFETs with various device layout geometries. Fig. 4 shows the schematic layout of a device with vertical body contacts. The body contacts were placed as vertical strips along the both sides of the device. The widths of the body contacts were the same as the height of the active region, which is denoted by W_f in Fig. 4. The distance from the outmost source junction to the vertical body contact is represented by d_v. Fig. 5 shows the values of R_{sub} when W_f varied from 1.5 μm to 10 μm with fixed d_v of 0.5 μm. R_{sub} were inversely proportional to W_f.

The MOSFETs with the vertical body contacts were also fabricated with d_v varying from 0.5 μm to 8 μm. The intrinsic devices were laid out identically and W_f were fixed at 2.5 μm. The extracted R_{sub} are plotted as a function of d_v in Fig. 6. R_{sub} increased linearly with d_v. The results show that the extracted values of R_{sub} are scalable with the geometric parameters.

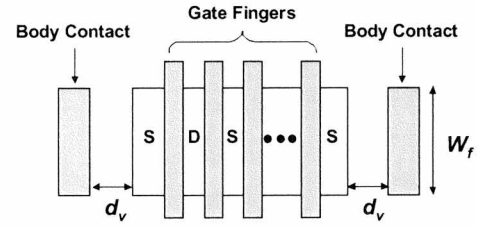

Fig. 4. Schematic layout of the device with vertical body contacts. W_f is the width of the gate-finger, which is the same with that of the body contact. d_v is the distance from the outmost source junction to the vertical body contact.

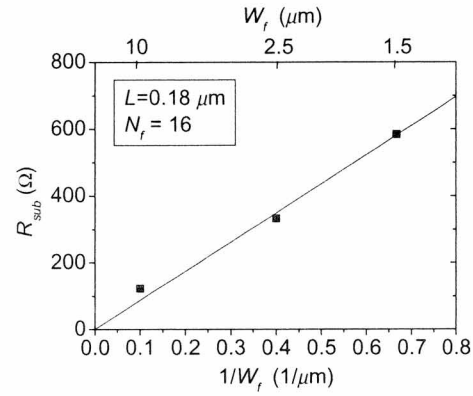

Fig. 5. R_{sub} as a function of $1/W_f$.

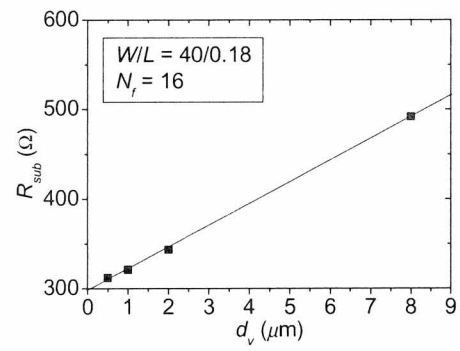

Fig. 6. R_{sub} for the devices with the vertical body contacts as a function of d_v.

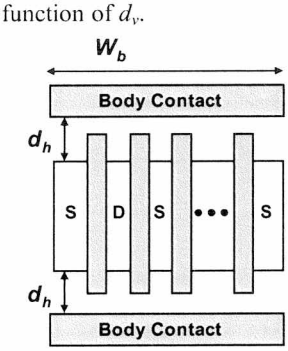

Fig. 7. Schematic layout of the device with horizontal body contacts. W_b is the width of the body contact. d_h is the distance from the outmost junction to the body contact.

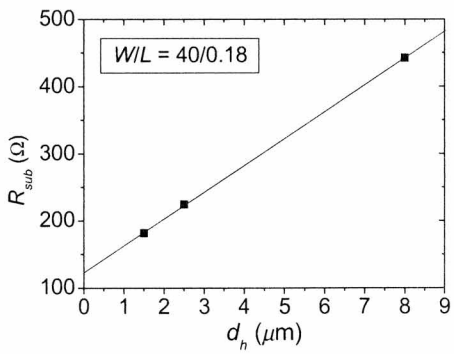

Fig. 8. R_{sub} for the devices with the horizontal body contacts as a function of d_h.

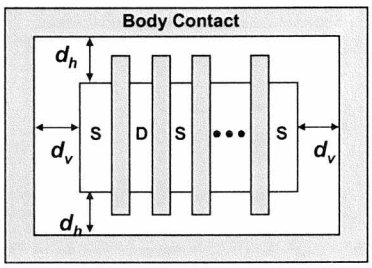

Fig. 9. Schematic layout of the device with a surrounding body contact. d_v is the distance from the outmost source junction to the vertical side of the body contact. d_h is the distance from the outmost junction to the horizontal side of the body contact.

R_{sub} were also extracted for the devices with horizontal body contacts. Fig. 7 shows the schematic layout of the device. The distance to the horizontal body contact is denoted by d_h. Fig. 8 presents R_{sub} as a function of d_h, when d_h varied from 1.5 μm to 8 μm, and N_f was 16. R_{sub} also increased linearly with d_h.

Fig. 9 shows the schematic layout of a device with a surrounding body contact. The distances from the outmost junctions to the vertical and the horizontal sides of the contact are d_v and d_h, respectively. The extracted R_{sub} were listed in Table. 1. The values calculated from the following equation were also shown in Table. 1.

$$R_{sub}(surr.cnt, d_v, d_h) = R_{sub}(ver.cnt, d_v) // R_{sub}(hor.cnt, d_h) \,. \quad (6)$$

d_v	0.5 μm	1 μm	20 μm
d_h	1.5 μm	2.5 μm	30 μm
Extracted R_{sub} (vertical contact, d_v)	312 Ω	322 Ω	547 Ω
Extracted R_{sub} (horizontal contact, d_h)	182 Ω	224 Ω	718 Ω
R_{sub} (Eq.(12))	115 Ω	132 Ω	311 Ω
Extracted R_{sub} (surrounding contact, d_v, d_v)	133 Ω	156 Ω	325 Ω

Table. 1. R_{sub} extracted from the device with a surrounding body contact, and R_{sub} calculated from (6).

The values of R_{sub} for the devices with the surrounding body contact were close to those calculated from (6) with less than 15% error. This implies that a surrounding body contact can be considered as a parallel combination of vertical body contacts and horizontal body contacts.

5 SIGNAL COUPLING THROUGH R_{sub}

At high frequencies, the four-terminal MOSFET with substrate parasictics has significant signal coupling through the substrate *R-C* network. In strong inversion region, the substrate signal coupling mainly affects the small-signal output characteristics [2], [7].

5.1 Modeling and Analysis

Fig. 10 shows the schematic of a one-substrate-resistor model. In the development of the analytical equations in this section, the effects of the parasitic resistances in gate, source, and drain terminals are assumed to be de-embedded to focus on the analysis of substrate signal coupling. The intrinsic RF MOSFET shown in Fig. 10 can be completely modeled with nine independent *y*-parameters [8].

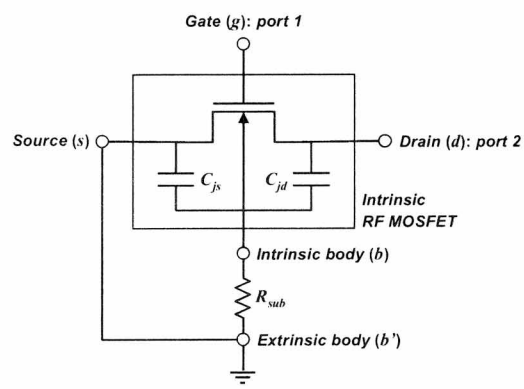

Fig. 10. Schematic of a one-substrate-resistor model.

Analyzing this model in terms of two-port *Y*-parameters results in the analytical expressions for Y_{22}. The real and imaginary parts of Y_{22} have large number of terms, but after careful examination of each term and taking only the significant terms, the following equations are obtained.

$$\mathrm{Re}(Y_{22}) \approx \mathrm{Re}(y_{dd}) + \frac{1}{1+\omega^2 R_{sub}^2 C_B^2} \times \underbrace{[\omega^2 g_{mb} R_{sub}{}^2 C_B (C_{bd}+C_{jd})}_{\text{term } A} + \underbrace{\omega^2 R_{sub}(C_{bd}+C_{jd})(C_{db}+C_{jd})]}_{\text{term } B} \quad (7)$$

$$\mathrm{Im}(Y_{22}) \approx \mathrm{Im}(y_{dd}) + \frac{1}{1+\omega^2 R_{sub}^2 C_B^2} \times \underbrace{[\omega g_{mb} R_{sub}(C_{bd}+C_{jd})}_{\text{term } C} - \underbrace{\omega^3 R_{sub}{}^2 C_B (C_{bd}+C_{jd})(C_{db}+C_{jd})]}_{\text{term } D} \quad (8)$$

where $C_B = C_{gb} + C_{bs} + C_{bd} + C_{gb0} + C_{js} + C_{jd}$.

In Eqs. (7) and (8), there are two types of coupling terms : the terms containing g_{mb} and those not containing g_{mb}. The former makes an influence on Y_{22} mainly in the strong inversion region because g_{mb} has a strong gate bias dependence and is nearly zero below threshold voltage [9], while the latter affects Y_{22} for all operation regions.

5.2 Measured Results and Discussions

The *S*-parameters of two RF MOSFETs were measured. Channel length and width of the devices were 0.18 μm and 40 μm, respectively. The measured devices were laid out identically except that their body contacts were placed at different distances from their outermost source junctions. Their DC characteristics were measured and verified to be exactly the same. The parasitic resistances in gate, source, and drain terminals were determined and removed by using the technique reported in [10]. Extracted values of R_{sub} are 38 Ω for the device with close body contacts and 285 Ω for the device with body contacts far from its outermost source junctions.

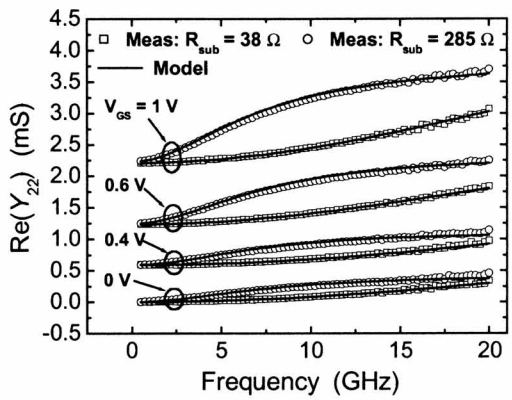

Fig. 11. Re(Y_{22}) of two measured MOSFETs at V_{DS} = 1 V. For clarity, the curves measured at V_{GS} = 0.4, 0.6, and 1 V were shifted by 0.5, 0.6 and 0.5 mS, respectively.

Fig. 11 compares Re(Y_{22})'s of the two devices. We can observe that the difference between Re(Y_{22})'s of two devices becomes larger as gate voltage increases. It is because the effect of the term A in Eq. (7) becomes significant with increasing gate voltage due to larger g_{mb}. The discrepancy at V_{GS} = 0 V is wholly due to the effect of the term B in Eq. (7). At low frequencies, Re(Y_{22}) of the device having large R_{sub} increases more rapidly than that of the device having small R_{sub} does. However, as frequency increases, the term $\omega^2 R_{sub}^2 C_B^2$ in the denominator of Eq. (7) starts to be dominant, and therefore Re(Y_{22}) for large R_{sub} increase more slowly than that for small R_{sub}. It can be seen that the results calculated using Eq. (7) agree very well with the measurement results. All the parameters (including the intrinsic parameters such as g_{ds} and C_{gd}) were extracted to verify the validity of the developed theory. Similar results were obtained for Im(Y_{22}).

6 CONCLUSION

A simple and accurate method was presented for extracting R_{sub} of RF MOSFETs of which the substrate is represented by a single resistor. The proposed gate voltage to extract R_{sub} is about 0 V, where the intrinsic components of the MOSFETs are negligible. The bias dependence and the geometry dependence of R_{sub} were also extracted and presented. The extracted values of R_{sub} are scalable with the geometric parameters. Signal coupling effect through R_{sub} was also analyzed.

ACKNOWLEDGMENTS

This work was partially supported by the National Program for Tera-level Nano Devices through MOST and by the System IC 2010 project.

REFERENCES

[1] J. J. Ou, X. Jin, I. Ma, C. Hu, and P. R. Gray, "CMOS RF Modeling for GHz Communication IC's", *Symp. VLSI Tech.*, pp. 94-95, 1998.

[2] S. H-M. Jen, C. C. Enz, D. R. Pehlke, M. Schröter, and B. J. Sheu, "Accurate Modeling and Parameter Extraction for MOS Transistors Valid up to 10 GHz", *IEEE Trans. Electron Devices*, vol.46, no.11, pp.2217-2227, 1999.

[3] R. Sung, P. Bendix, and M. B. Das, "Extraction of High-frequency Equivalent Circuit Parameters of Submicron Gate-length MOSFETs", *IEEE Trans. Electron Devices*, vol. 45, no.8, pp.1769-1775, 1998.

[4] L. Tiemeijer and D. Klaassen, "Geometry Scaling of the Substrate Loss of RF MOSFETs", *in Proc. European Solid-State Device Research Conf.*, pp. 480-483, 1998.

[5] S. F. Tin, A. A. Osman, K. Mayaram, and C. Hu, "A Simple Subcircuit Extension of the BSIM3v3 Model for CMOS RF Design", *IEEE J. Solid-State Circuits*, vol.35, no. 4, pp.612–624, 2000.

[6] Y. Cheng and M. Matloubian, "On the High-frequency Characteristics of Substrate Resistance in RF MOSFETs", *IEEE Electron Device Letters*, vol. 21, pp. 604–606, 2000.

[7] I. Kwon, M. Je, K. Lee, and H. Shin, "A Simple and Analytical Parameter Extraction Method of MOSFET for Microwave Modeling," *IEEE Trans. Microwave Theory and Techniques*, vol. 50, pp. 1503-1509, 2002.

[8] M. Bagheri and Y. Tsividis, "A Small Signal DC-to-High-Frequency Nonquasistatic Model for the Four-Terminal MOSFET Valid in All Regions of Operation," *IEEE Trans. Electron Deviecs*, vol. ED-32, pp. 2383–2391, 1985.

[9] Y. Tsividis, *Operation and Modeling of the MOS Transistor*, 2nd ed., McGraw-Hill, 1999.

[10] A. Pascht, M. Grozing, D. Wiegner, and M. Berroth, "Small-Signal and Temperature Noise Model for RF MOSFETs," *IEEE Trans. Microwave Theory and Techniques*, vol. 50, pp. 1927–1934, 2002.